Published in final edited form as:

J Clin Periodontol. 2015 July ; 42(7): 599–608. doi:10.1111/jcpe.12415.

Ac45 silencing mediated by AAV-sh-Ac45-RNAi prevents both bone loss and inflammation caused by periodontitis

Zheng Zhu[1,2,#], **Wei Chen**[2,#], **Liang Hao**[2], **Guochun Zhu**[2], **Yun Lu**[2], **Sheng Li**[1,2], **Lin Wang**[1,*], and **Yi-Ping Li**[2,*]

[1]Jiangsu Key Laboratory of Oral Diseases, Nanjing Medical University; Affiliated Hospital of Stomatology, Nanjing Medical University, Nanjing 210029, People's Republic of China

[2]Department of Pathology, University of Alabama at Birmingham, Birmingham, AL 35294, USA

Abstract

Aim—Periodontitis induced by oral pathogens leads to severe periodontal tissue damage and osteoclast-mediated bone resorption caused by inflammation. Based on the importance of Ac45 in osteoclast formation and function, we performed this study to evaluate the therapeutic potential of periodontitis by local adeno-associated virus (AAV)-mediated Ac45 gene knockdown.

Material and Methods—We used AAV-mediated short hairpin RNAi knockdown of Ac45 gene expression (AAV-sh-Ac45) to inhibit bone erosion and gingival inflammation simultaneously in a well-established periodontitis mouse model induced by *Porphyromonas gingivalis W50*. Histological studies were performed to evaluate the bone protection of AAV-sh-Ac45. Immunochemistry, ELISA and qRT-PCR were performed to reveal the role of Ac45 knockdown on inflammation, immune response and expression of cytokine.

Results—We found that Ac45 knockdown impaired osteoclast-mediated extracellular acidification and bone resorption *in vitro and in vivo*. Furthermore, local administration of AAV-sh-Ac45 protected mice from bone erosion by >85% and attenuated inflammation and decreased infiltration of T-cells, dendritic cells and macrophages in the periodontal lesion. Notably, the expression of pro-inflammatory cytokines was also reduced.

Conclusions—Local AAV-sh-Ac45 gene therapy efficiently protects against periodontal tissue damage and bone erosion through both inhibition of osteoclast function and attenuating inflammation, and may represent a powerful new treatment strategy for periodontitis.

Keywords

AAV-mediated RNAi knockdown; gene therapy; Ac45; periodontal disease; osteoclast immunology; gingival inflammation; alveolar bone resorption

[*]**Correspondence address:** Yi-Ping Li, PhD, Department of Pathology, University of Alabama at Birmingham, Birmingham, AL 35294, USA; Tel: 205-975-2606, Fax: 205-975-4919, ypli@uab.edu and Lin Wang, PhD, DDS, College of Stomatology, Nanjing Medical University, Nanjing 210029, People's Republic of China; Tel: 025-85031865, Fax: 025-86516414, LW603@njmu.edu.cn.
[#]The authors contributed equally.

The authors declare that they have no conflict of interests.

Introduction

Periodontal disease affects about 80% of adults in America (Saraiva et al., 2007, Albandar, 2002), and is characterized by oral bacterial infection-induced gingival inflammation, oral bone resorption, and tooth loss. Periodontitis is also associated with other diseases such as rheumatoid arthritis (Wolff et al., 2014, Demmer et al., 2011), diabetes (Lalla and Papapanou, 2011), and heart disease (Schaefer et al., 2009). Although many efforts have been made to develop effective therapies for periodontitis, none have been very effective and there is still an urgent need for better treatments and preventative strategies.

The chronic inflammation of periodontal disease is induced by polymicrobial infection, with a prominent pathogen being *Porphyromonas gingivalis W50 (P. gingivalis W50)*. The pathogenesis of periodontal disease involves bacterial biofilms that develop on the tooth surface and within the gingival crevice, which induces a host inflammatory response in the gingival tissues. The response results in osteoclast-mediated bone loss and the subsequent loss of teeth.

Osteoclasts are able to decrease the pH at the interface with bone via a multi-unit Vacuolar-type H^+-ATPases (V-ATPases) complex, which is necessary for osteoclast mediated bone resorption (Jefferies et al., 2008, Inoue et al., 2003, Xiao et al., 2008). V-ATPases are primarily responsible for proton secretion and intracellular vesicle acidification. It has been suggested that V-ATPases are involved in a wide variety of physiological processes, including endocytosis, exocytosis, intracellular membrane trafficking, membrane fusion, and cell–cell fusion (Jefferies et al., 2008).

Ac45 (Atp6ap1), an accessory subunit of the V-ATPase complex, is a type I transmembrane protein associated with the V-ATPase membrane domain (V0) (Yang et al., 2012). The domains located in the N- and C-terminal portions of the Ac45 protein direct its trafficking, V-ATPase recruitment and $Ca2^+$ dependent-regulated exocytosis (Jansen et al., 2012). Recently, overexpression of an Ac45 cytoplasmic terminus deletion mutant in RAW264.7 cells resulted in a dramatic reduction in osteoclast mediated bone resorption and alterations in the binding proximity of Ac45 with the V-ATPase V0 domain subunits a3, c”, and d (Yang et al., 2012). Using a siRNA-based approach, it was shown that targeted suppression of Ac45 impairs intracellular acidification and endocytosis; both are prerequisites for osteoclastic bone resorptive function in vitro (Qin et al., 2011). Notably, Ac45 knockdown in osteoclasts exhibited impaired lysosomal trafficking and exocytosis, as indicated by the absence of lysosomal trafficking to the ruffled border and a lack of cathepsin K exocytosis into the resorption lacuna (Yang et al., 2012). There is also growing recognition that osteoclasts are immune cells with roles in immune responses beyond mediating the bone destruction that can accompany them (Boyce, 2013).

The aim of the current investigation is to conclusively determine the therapeutic potential of silencing Ac45 *in vivo* using AAV-sh-Ac45, to reduce alveolar bone erosion, and inflammation in periodontal lesions in a well-established periodontitis mouse model. The AAV silencing approach is a relatively new and effective tool but is safe and well tolerated by patients with advanced Parkinson's disease (Kaplitt et al., 2007), suggesting that *in vivo*

gene therapy is practical and causes only a very mild immune response to the AAV vector. Therefore, in this study we used the AAV RNAi knockdown system to investigate the therapeutic potential of *Ac45* silencing due to its unique attributes as described.

Materials and Methods

For complete Materials and Methods, please see Supplementary Material

Ethics Statement

All experimental protocols were approved by the NIH and the Institutional Animal Care and Use Committee (IACUC) of the University of Alabama at Birmingham (UAB) and completed within 16 weeks after birth (Sasaki et al., 2008). Approval for the animal protocol related to this study (Animal Protocol Number 121209236) was renewed by UAB IACUC on December 10, 2012.

Animals

Eight-week-old female wild-type (WT) BALB/cJ mice (Jackson Laboratory) were used for this study. Mice were divided into 3 groups: (1) Normal group (no *P. gingivalis W50* infection) (n=5 mice); (2) *P. gingivalis W50* infection and AAV-shRNA-Ac45 (hereafter referred to as AAV-sh-Ac45) treatment (n=5); (3) *P. gingivalis W50* infection and AAV-sh-luc-YFP treatment (disease group) (n=5). The experiments were performed in triplicate on three independent occasions, resulting in a total sample number of n=15 for each group.

Design and construction of short hairpin ribonucleic acid (shRNA)

Using the Dharmacon siDESIGN Centre (http://www.dharmacon.com) (Feng et al., 2009), we generated shRNA that would target Ac45. As a control vector, we used AAV-H1-shRNA-luc-YFP (gift from Dr. Sonoko Ogawa), which contains a luciferase-specific shRNA and a yellow fluorescent protein (YFP) cassette (Alexander et al., 2010). AAV-H1 contains a human Pol III H1 promoter for expression of shRNA as well as an independent green fluorescent protein (EGFP) expression cassette (Musatov et al., 2006). We cloned the H1 promoter shRNA expression cassette into the AAV construct as described (Yang et al., 2007, Wilensky et al., 2009). The following shRNA oligonucleotides were annealed and cloned downstream of the H1 promoter of AAV-H1 into BglII and Xbal sites to produce AAV-H1-shRNA-Ac45: 5’ GATCCCCCCTTGCTGTTTATAGTGCTTT**TTCAAGAGA**AAAGCACTATAAACAGCAAGGTTTTTGGAAT-3’. Nucleotides specific for targeting Ac45 are underlined. The bold type signifies the 9-base pair hairpin spacer.

Infection with *Porphyromonas gingivalis W50* strains

Oral inoculation was achieved using 20μl of the PBS mixture containing 10^{10} bacteria/ml *P. gingivalis W50* (ATCC: 53978) and 2% CMC (Jiang et al., 2013). The periodontal infection regimen was conducted according to a previously described protocol (Yang et al., 2013) (with modifications. In brief, all animals received antibiotic treatment for three days to reduce the original oral flora, followed by three days of an antibiotic-free period prior to oral inoculation with a dental micro-brush once per day for four consecutive days.

AAV-shRNA-Ac45 transduction of *P. gingivalis W50* infected mice

We injected AAV-sh-*Ac45* in a site-specific manner as described previously (Jiang et al., 2013). In addition, we also made some modifications. Starting 4 days after the initial infection and continuing for 5–7 consecutive days, mice were anesthetized and injected approximately 0.3–0.5 mm above the gingival margin of the maxillary molars on the palatal aspects with 3 μl containing 2×10^9 packaged genomic particles in PBS, of either AAV-sh-Ac45 or AAV-sh-luc-YFP viral vector using 50 μl Hamilton syringe attached to a microinfusion pump (World Precision Instruments, Sarasota, FL).

Harvest and preparation of tissue samples

Animals were sacrificed by CO_2 inhalation 55 days after initial infection. The maxillae were hemisected. For bone height measurements, five samples from the left side were defleshed in 2.6% sodium hypochlorite (Trepagnier et al., 1977) for 30–40 minutes, rinsed in tap water three times, placed in 70% alcohol, stained with 0.2% methylene blue, and mounted on microscope slides for bone loss measurements. Five samples from the right side were immediately fixed in 4% paraformaldehyde and prepared for histological analysis according to standard protocol. In brief, samples for paraffin sections were fixed in 4% formaldehyde for 24 hours, washed with PBS, decalcified in 10% EDTA in 0.1M TRIS solution (PH=7.0) for 21 days (replenished each day), washed with 1XPBS three times, and embedded in paraffin after series dehydration. Gingival tissues and/or alveolar bone were isolated under a surgical microscope. Gingival tissues and alveolar bone from five samples were pooled for qRT-PCR, and gingival tissues from another five samples were pooled for ELISAs for cytokines. These experiments were repeated three times.

Western blotting analysis

Western blotting was performed as previously outlined (Chen et al., 2013) and visualized and quantified using a Fluor-S Multi-Imager with Multi-Analyst software (Bio-Rad). A mouse anti-Ac45 monoclonal antibody (Santa Cruz, Dallas, TX) was used at a 1:1000 dilution, with goat anti-mouse IgG-HRP (7076S, Cell signaling) used at a 1:5000 dilution to visualize the reaction.

Histological analysis

Samples were fixed in 4% paraformaldehyde for 24 hours, decalcified in 10% EDTA for 10 days, and embedded in paraffin or processed as frozen sections (Hao et al., 2015, Gao et al., 2013). H&E (Hematoxylin and eosin) staining and TRAP (Tartrate-resistant acid phosphatase ate-resistant acid phosphatase) staining were performed by standard methods.

Immunohistochemistry and Immunofluorescence analysis

We performed immunohistochemistry analysis by using goat polyclonal anti-Ac45 primary antibody (Santa Cruz, Dallas, TX), mouse monoclonal anti-Ctsk (Cathepsin K) primary antibody (Santa Cruz, Dallas, TX) and rat monoclonal anti-F4/80 primary antibody (eBioscience, San Diego, CA) (Chen et al., 2014). VECTASTAIN Elite ABC-Peroxidase Kits along with a DAB kit (Vector Laboratories, Burlingame, CA) as a substrate were used for the peroxidase-mediated reaction. Immunofluorescence analysis was performed as

outlined previously (Jiang et al., 2013), with the exception that we used Armenian hamster monoclonal anti-CD11c (Abcam, Cambridge, MA) as the primary antibody and Fluorescein Iso-thiocyanate (FITC)-labeled secondary antibody.

Real-time quantitative PCR (qRT-PCR)

The experiment was done in accordance with the MIQE guidelines. We included 5 tissue samples each group. RNA extraction was carried out under standard procedures using Trizol (Invitrogen) (Chen et al., 2007, Li et al., 1996). The extracted RNA was reverse transcribed using Vilo® Master Kit (Invitrogen). qRT-PCR was performed as described (Allaire et al., 2011) using SYBR® Green primers purchased from Invitrogen as listed in Table 1 according to the manufacturer's instructions. The mRNA expression level of the housekeeping gene β-actin was used as an endogenous control and enabled calculation of specific mRNA expression levels as a ratio of β-actin (delta CT). The CT value of HPRT and β-actin was compared to select better endogenous control as described (Silver et al., 2006).

Enzyme-linked immunosorbent assay (ELISA)

For protein extraction, the frozen periodontal tissue samples were homogenized in 1 ml of lysis buffer. The mixture was incubated at 4°C for 1 hour, and the supernatant was collected after centrifugation and stored at −80 °C until assay. ELISA was carried out in accordance with the manufacturer's instructions. Results were expressed as pg cytokine/mg tissue.

Statistical analysis and data quantification analysis

Experimental data were reported as mean ± SD. All experiments were performed in triplicate on three independent occasions. *In vitro* osteoclast and bone resorption data were analyzed with the Student's t-test. Bone loss measurements, histological and immunohistochemical measurements, qRT-PCR, and ELISA data were analyzed by ANOVA. P values <0.05 were considered significant.

Results

AAV-sh-Ac45 efficiently knocked down expression of Ac45 and impaired osteoclast-mediated extracellular acidification and bone resorption *in vitro*

To evaluate the effect of inhibition of Ac45 on bone erosion, we generated shRNA that targeted the expression of this gene. Cell fluorescence indicated that efficient transduction of pre-osteoclasts and osteoclasts with AAV-sh-Ac45 or AAV-sh-luc-YFP was achieved using a titer of approximately 6×10^{11} DNase resistant particles (DRP)/ml (Fig. 1A). We performed Western blot analysis, and found that osteoclasts transduced with AAV-sh-Ac45 have an approximately 75% reduction in Ac45 expression compared to osteoclasts transduced with AAV-sh-luc-YFP (Fig. 1B, C). These results indicate that AAV-sh-Ac45 targets Ac45 mRNA efficiently and reduces Ac45 protein expression.

As expected, we found that osteoclasts transduced with AAV-sh-Ac45 show reduced extracellular acidification compared to osteoclasts transduced with AAV-sh-luc-YFP (Fig. 1D), demonstrating the specificity of the Ac45 inhibition. TRAP positive cells were reduced

in osteoclasts transduced with AAV-sh-Ac45 compared to that with AAV-sh-luc-YFP (Fig. 1D). Bone resorption was analyzed by using wheat germ agglutinin (WGA) and scanning electron microscopy (SEM) to visualize resorption pits on bone (Fig. 1D). As shown, AAV-mediated knockdown of Ac45 was highly effective in preventing bone resorption compared to the control group ($p<0.005$; Fig. 1E).

AAV effectively transduced periodontal tissue and down regulated Ac45 expression leading to reduction of bone resorption in *P. gingivalis W50*-stimulated periodontitis

Following local injection with AAV-sh-Ac45, EGFP expression was observed in gingival tissue, periodontal ligament, dental pulp, indicating that AAV-sh-Ac45 effectively diffuses throughout periodontal tissues (Fig. 2A). We performed anti-Ac45 immunohistochemistry staining and found that AAV-sh-Ac45 treatment notably reduced expression of Ac45 *in vivo* (Fig. 2G). There was no significant difference in bone loss between the normal group and the AAV-sh-Ac45 treatment group ($p>0.05$). However, the AAV-sh-luc-YFP treatment group had significantly more bone loss compared to the AAV-sh-Ac45 group or the normal group ($p<0.01$) (Fig. 2B, C). Indeed, AAV-mediated Ac45 knockdown largely protected mice from *P. gingivalis W50* infection-stimulated bone erosion (>85%) (Fig. 2B, C). We also found that TRAP positive cells and Ctsk expression was reduced in AAV-sh-Ac45 treated mice compared to AAV-sh-luc-YFP (Fig. 2E, F). These results indicate that *Ac45* depletion protects against *P. gingivalis W50*-stimulated bone erosion in the mouse model of periodontitis.

AAV-mediated *Ac45* knockdown decreased bone erosion and the number of T-cells in the periodontal area

In order to determine if the periodontal ligament between the tooth root and the bone is normalized by AAV-sh-Ac45 treatment, we examined hematoxylin & eosin-stained sections. It was determined that the distance between the tooth root surface and the alveolar bone is about doubled in the control AAV-sh-luc-YFP treatment group compared to the normal and AAV-sh-Ac45 treatment groups (Fig. 3A–C), indicating that AAV-sh-Ac45 prevents periodontal ligament damage and alveolar bone loss. To investigate the effect of AAV-sh-Ac45 on T-cells *in vivo*, alveolar sections were subjected to immunofluorescence staining using the CD3 antibody to detect T-cells (Fig. 4A, B). Our results showed that the number of CD3 expressing T-cells in the periodontal lesions was significantly reduced in the AAV-sh-Ac45 treatment group compared to that of the AAV-sh-luc-YFP treatment group (Fig. 4C).

AAV-mediated Ac45 knockdown decreased the number of dendritic cells and macrophages in the periodontal area

The results of immunofluorescence staining showed that the number of CD11c expressing dendritic cells in the periodontal area was significantly reduced in the AAV-sh-Ac45 treatment group compared to that of the AAV-sh-luc-YFP treatment group (Fig. 5A–C). By performing immunohistochemistry staining, we found that the number of F4/80 expressing macrophages in the periodontal lesions was significantly reduced in the AAV-sh-Ac45 treatment group compared to that of the AAV-sh-luc-YFP treatment group (Fig. 5D–F).

AAV-sh-*Ac45* reduced the expression of pro-inflammatory cytokines in the periodontal tissues toward normal expression levels

The AAV-sh-Ac45 treatment group had significantly lower mRNA expression of the inflammatory mediators Interleukin-1 (IL-1), IL-6, IL-17α, tumor necrosis factor-α (TNF-α), and RANKL compared to the AAV-sh-luc-YFP group ($p<0.05$). Interestingly, the OPG mRNA expression was increased in the AAV-sh-Ac45 group (Fig. 6A). The ELISA results showed that infected AAV-sh-luc-YFP groups had elevated levels of IL-1α, IL-12α, IL-17α, and TNF-α, but decreased the level of IL-10 compared to uninfected controls. However, in all cases, the elevated levels of these mediators were lower in the AAV-sh-*Ac45* treatment group compared to the AAV-sh-luc-YFP group (Fig. 6B).

Discussion

In the present study, we demonstrated that AC45 gene silencing by AAV-sh-Ac45 inhibited Ac45 expression and dramatically reduced periodontal disease progression. AAV-sh-Ac45 local injection impaired osteoclast mediated bone resorption through inhibition of osteoclast function, reducing osteoclast numbers and pro-inflammatory cytokine expression, furthermore protected mice from *P. gingivalis W50*-stimulated periodontal bone loss *in vivo* by 85%.

We found that Ac45 expression levels were efficiently decreased in the AAV-sh-Ac45 treatment group both *in vitro* and *in vivo*. As a result of Ac45 knockdown, osteoclasts may form normal actin rings, but had severely impaired extracellular acidification and bone resorption. Of interest, osteoclast numbers were also decreased in the AAV-sh-Ac45 treatment group, as indicated by reduced TRAP staining, and reduced expression of Cathepsin K. In our study, the expression level of RANKL mRNA was reduced in the AAV-sh-Ac45 treatment group. In contrast, the expression level of OPG mRNA was increased in the AAV-sh-Ac45 treatment group. The RANK/RANKL/OPG signaling pathway is essential for osteoclastogenesis (Boyce and Xing, 2007, Wright et al., 2009). The change in RANKL and OPG expression was consistent with osteoclast numbers and bone resorption reduction in the AAV-sh-Ac45 group.

Interestingly, we found that mononuclear cell infiltration in the AAV-sh-Ac45 group was significantly decreased compared with the AAV-sh-luc-YFP group, suggesting that knockdown of Ac45 potentially affects immunity and inflammation in the periodontal lesion. Therefore, we performed immunohistochemistry and immunofluorescence staining to observe whether there were changes on immune response. ELISA and qRT-PCR were also performed to detect the protein and RNA levels of related inflammatory mediators. It has been reported that T and B lymphocytes are major sources of RANKL in the bone resorptive lesion of periodontitis (Kawai et al., 2006), and our finding that CD3+ T-cell numbers were reduced in periodontal lesions in the AAV-sh-Ac45 treatment group is consistent with this observation (Fig. 4B). There were also fewer macrophages and CD11c+ dendritic cells in the periodontal lesions in the AAV-sh-Ac45 group than in the AAV-sh-Luc-YFP group (Fig. 5A, B). To our knowledge, there is currently no literature that suggests that Ac45 expressed in T cells, dendritic cells or macrophages. In our study, the expression of Cathepsin K was reduced as a result of Ac45 knockdown. Cathepsin K was first discovered and cloned by our

lab (Li et al., 1995), which was reported to play important function in immune cells (Hao et al., 2015). Additional studies are needed to distinguish between these possibilities. The capacity of AAV-sh-Ac45 treatment to dramatically reduce inflammation and bone erosion in infected mice was observed after infection. The effect of AAV-sh-Ac45 on osteoclast numbers may represent a direct effect on osteoclast precursor cell proliferation and fusion but also may result indirectly from inhibition of T-cell activation and inflammation.

The protein expression level of pro-inflammatory cytokines, including TNF-α, IL-1, IL-6, IL-12 and IL-17A, was reduced in the AAV-sh-Ac45 group and the results were consistent with the mRNA level detected by qRT-PCR. These findings were consisted with the CD3+ T-cell numbers and inflammation reduction by Ac45 knockdown. It has been demonstrated that IL-1, IL-6, and TNF-α may regulate proliferation and differentiation of mononuclear preosteoclasts into osteoclast progenitors and fusion of the preosteoclasts into multinucleated osteoclasts (Braun and Zwerina, 2011, Zhao and Ivashkiv, 2011). As a potent anti-inflammatory cytokine that suppresses both immunoproliferative and inflammatory responses, IL-10 downregulates the synthesis of pro-inflammatory cytokines and chemokines, such as IL-1, IL-6, and TNF-α (Houri-Haddad et al., 2007, Mosser and Zhang, 2008). Previous study also showed that IL-10 will increase the B-cell proliferation with the presence of bacteria, which indicated that IL-10 may have biphasic function during the immune response in periodontitis lesion area (Champaiboon et al., 2000). In our study, we found that the mRNA level of IL-10 increased in the AAV-sh-Ac45 group. This result was also consistent with recent studies which have indicated that IL-10 can contribute to the maintenance of bone mass through inhibition of osteoclastic bone resorption and regulation of osteoblastic bone formation (Owens et al., 1996, Park-Min et al., 2009, Zhang and Chen, 2014).

Current clinical therapies for periodontal disease have been focused on anti-microbial treatments as well as surgery, which generally have limited efficacy. In contrast, AAV-sh-Ac45 gene therapy to anti-bone erosion and anti-inflammation has achieved an outcome that other technology may not be able to accomplish. Gene transfer with AAV2 has been shown to be safe and effective in a number of disease models (Gombash et al., 2013, Xu et al., 2014, Pien et al., 2009). In periodontal disease, AAV2 achieved the highest transduction rates for human primary periodontal ligament cells as well as periodontal tissues (Kunze et al., 2009). Based on our study, we believe that AAV-mediated Ac45 knockdown can be employed as a novel and effective periodontitis therapy.

Supplementary Material

Refer to Web version on PubMed Central for supplementary material.

Acknowledgements

We thank Ms. Suzy Newton for their excellent assistance with the manuscript. We also thank Drs. Sergei Musatov and Sonoko Ogawa for kindly providing the AAV-H1-shRNA-luc-YFP and AAV-H1 vectors and helpful suggestions. We appreciate the assistance of the Center for Metabolic Bone Disease at the University of Alabama at Birmingham (P30 AR046031). We are also grateful for the assistance of the Small Animal Phenotyping Core, Metabolism Core, Histomorphometry and Molecular Analyses Core, Neuroscience Image Core, and Neuroscience

Molecular Detection Core Laboratory at the University of Alabama at Birmingham (P30 NS0474666). This study was supported by NIH grants AR-44741 (Y.P.L.) and R01DE023813 (Y.P.L.).

Reference

Albandar JM. Periodontal diseases in North America. Periodontol 2000. 2002; 29:31–69. [PubMed: 12102702]

Alexander B, Warner-Schmidt J, Eriksson T, Tamminga C, Arango-Lievano M, Ghose S, Vernov M, Stavarache M, Musatov S, Flajolet M, Svenningsson P, Greengard P, Kaplitt MG. Reversal of depressed behaviors in mice by p11 gene therapy in the nucleus accumbens. Sci Transl Med. 2010; 2:54ra76.

Allaire JM, Darsigny M, Marcoux SS, Roy SA, Schmouth JF, Umans L, Zwijsen A, Boudreau F, Perreault N. Loss of Smad5 leads to the disassembly of the apical junctional complex and increased susceptibility to experimental colitis. Am J Physiol Gastrointest Liver Physiol. 2011; 300:G586–G597. [PubMed: 21212325]

Boyce BF. Advances in the regulation of osteoclasts and osteoclast functions. J Dent Res. 2013; 92:860–867. [PubMed: 23906603]

Boyce BF, Xing L. Biology of RANK, RANKL, and osteoprotegerin. Arthritis Res Ther. 2007; 9(Suppl 1):S1. [PubMed: 17634140]

Braun T, Zwerina J. Positive regulators of osteoclastogenesis and bone resorption in rheumatoid arthritis. Arthritis Res Ther. 2011; 13:235. [PubMed: 21861862]

Champaiboon C, Yongvanitchit K, Pichyangkul S, Mahanonda R. The immune modulation of B-cell responses by Porphyromonas ginginvalis and interleukin-10. J Periodontol. 2000; 71:468–475. [PubMed: 10776936]

Chen W, Ma J, Zhu G, Jules J, Wu M, McConnell M, Tian F, Paulson C, Zhou X, Wang L, Li Y-P. Cbfβ deletion in mice recapitulates cleidocranial dysplasia and reveals multiple functions of Cbfβ required for skeletal development. Proceedings of the National Academy of Sciences of the United States of America. 2014; 111:8482–8487. [PubMed: 24850862]

Chen W, Yang S, Abe Y, Li M, Wang Y, Shao J, Li E, Li YP. Novel pycnodysostosis mouse model uncovers cathepsin K function as a potential regulator of osteoclast apoptosis and senescence. Hum Mol Genet. 2007; 16:410–423. [PubMed: 17210673]

Chen W, Zhu G, Hao L, Wu M, Ci H, Li Y-P. C/EBPα regulates osteoclast lineage commitment. Proceedings of the National Academy of Sciences. 2013; 110:7294–7299.

Demmer RT, Molitor JA, Jacobs DR Jr, Michalowicz BS. Periodontal disease, tooth loss and incident rheumatoid arthritis: results from the First National Health and Nutrition Examination Survey and its epidemiological follow-up study. J Clin Periodontol. 2011; 38:998–1006. [PubMed: 22092471]

Feng S, Deng L, Chen W, Shao J, Xu G, Li YP. Atp6v1c1 is an essential component of the osteoclast proton pump and in F-actin ring formation in osteoclasts. Biochem J. 2009; 417:195–203. [PubMed: 18657050]

Gao B, Chen W, Hao L, Zhu G, Feng S, Ci H, Zhou X, Stashenko P, Li YP. Inhibiting periapical lesions through AAV-RNAi silencing of cathepsin K. J Dent Res. 2013; 92:180–186. [PubMed: 23166044]

Gombash SE, Manfredsson FP, Kemp CJ, Kuhn NC, Fleming SM, Egan AE, Grant LM, Ciucci MR, MacKeigan JP, Sortwell CE. Morphological and behavioral impact of AAV2/5-mediated overexpression of human wildtype alpha-synuclein in the rat nigrostriatal system. PLoS One. 2013; 8:e81426. [PubMed: 24312298]

Hao L, Chen W, McConnell M, Zhu Z, Li S, Reddy M, Eleazer PD, Wang M, Li Y-P. A small molecule, Odanacatib, inhibits inflammation and bone loss caused by endodontic disease. Infect Immun. 2015

Houri-Haddad Y, Soskolne WA, Halabi A, Shapira L. IL-10 gene transfer attenuates P. gingivalis-induced inflammation. J Dent Res. 2007; 86:560–564. [PubMed: 17525358]

Inoue T, Wilkens S, Forgac M. Subunit structure, function, and arrangement in the yeast and coated vesicle V-ATPases. J Bioenerg Biomembr. 2003; 35:291–299. [PubMed: 14635775]

Jansen EJ, van Bakel NH, Olde Loohuis NF, Hafmans TG, Arentsen T, Coenen AJ, Scheenen WJ, Martens GJ. Identification of domains within the V-ATPase accessory subunit Ac45 involved in V-ATPase transport and Ca2+-dependent exocytosis. J Biol Chem. 2012; 287:27537–27546. [PubMed: 22736765]

Jefferies KC, Cipriano DJ, Forgac M. Function, structure and regulation of the vacuolar (H+)-ATPases. Arch Biochem Biophys. 2008; 476:33–42. [PubMed: 18406336]

Jiang H, Chen W, Zhu G, Zhang L, Tucker B, Hao L, Feng S, Ci H, Ma J, Wang L, Stashenko P, Li YP. RNAi-mediated silencing of Atp6i and Atp6i haploinsufficiency prevents both bone loss and inflammation in a mouse model of periodontal disease. PLoS One. 2013; 8:e58599. [PubMed: 23577057]

Kaplitt MG, Feigin A, Tang C, Fitzsimons HL, Mattis P, Lawlor PA, Bland RJ, Young D, Strybing K, Eidelberg D, During MJ. Safety and tolerability of gene therapy with an adeno-associated virus (AAV) borne GAD gene for Parkinson's disease: an open label, phase I trial. Lancet. 2007; 369:2097–2105. [PubMed: 17586305]

Kawai T, Matsuyama T, Hosokawa Y, Makihira S, Seki M, Karimbux NY, Goncalves RB, Valverde P, Dibart S, Li YP, Miranda LA, Ernst CW, Izumi Y, Taubman MA. B and T lymphocytes are the primary sources of RANKL in the bone resorptive lesion of periodontal disease. Am J Pathol. 2006; 169:987–998. [PubMed: 16936272]

Kunze M, Huber A, Krajewski A, Lowden E, Schuhmann N, Buening H, Hallek M, Noack M, Perabo L. Efficient gene transfer to periodontal ligament cells and human gingival fibroblasts by adeno-associated virus vectors. J Dent. 2009; 37:502–508. [PubMed: 19362764]

Lalla E, Papapanou PN. Diabetes mellitus and periodontitis: a tale of two common interrelated diseases. Nat Rev Endocrinol. 2011; 7:738–748. [PubMed: 21709707]

Li YP, Alexander M, Wucherpfennig AL, Yelick P, Chen W, Stashenko P. Cloning and complete coding sequence of a novel human cathepsin expressed in giant cells of osteoclastomas. J Bone Miner Res. 1995; 10:1197–1202. [PubMed: 8585423]

Li YP, Chen W, Stashenko P. Molecular cloning and characterization of a putative novel human osteoclast-specific 116-kDa vacuolar proton pump subunit. Biochem Biophys Res Commun. 1996; 218:813–821. [PubMed: 8579597]

Mosser DM, Zhang X. Interleukin-10: new perspectives on an old cytokine. Immunol Rev. 2008; 226:205–218. [PubMed: 19161426]

Musatov S, Chen W, Pfaff DW, Kaplitt MG, Ogawa S. RNAi-mediated silencing of estrogen receptor {alpha} in the ventromedial nucleus of hypothalamus abolishes female sexual behaviors. Proc Natl Acad Sci U S A. 2006; 103:10456–10460. [PubMed: 16803960]

Owens JM, Gallagher AC, Chambers TJ. IL-10 modulates formation of osteoclasts in murine hemopoietic cultures. J Immunol. 1996; 157:936–940. [PubMed: 8752948]

Park-Min KH, Ji JD, Antoniv T, Reid AC, Silver RB, Humphrey MB, Nakamura M, Ivashkiv LB. IL-10 suppresses calcium-mediated costimulation of receptor activator NF-kappa B signaling during human osteoclast differentiation by inhibiting TREM-2 expression. J Immunol. 2009; 183:2444–2455. [PubMed: 19625651]

Pien GC, Basner-Tschakarjan E, Hui DJ, Mentlik AN, Finn JD, Hasbrouck NC, Zhou S, Murphy SL, Maus MV, Mingozzi F, Orange JS, High KA. Capsid antigen presentation flags human hepatocytes for destruction after transduction by adeno-associated viral vectors. J Clin Invest. 2009; 119:1688–1695. [PubMed: 19436115]

Qin A, Cheng TS, Lin Z, Pavlos NJ, Jiang Q, Xu J, Dai KR, Zheng MH. Versatile roles of V-ATPases accessory subunit Ac45 in osteoclast formation and function. PLoS One. 2011; 6:e27155. [PubMed: 22087256]

Saraiva MC, Taichman RS, Braun T, Nriagu J, Eklund SA, Burt BA. Lead exposure and periodontitis in US adults. J Periodontal Res. 2007; 42:45–52. [PubMed: 17214639]

Sasaki H, Suzuki N, Kent R Jr, Kawashima N, Takeda J, Stashenko P. T cell response mediated by myeloid cell-derived IL-12 is responsible for Porphyromonas gingivalis-induced periodontitis in IL-10-deficient mice. J Immunol. 2008; 180:6193–6198. [PubMed: 18424741]

Schaefer AS, Richter GM, Groessner-Schreiber B, Noack B, Nothnagel M, El Mokhtari NE, Loos BG, Jepsen S, Schreiber S. Identification of a shared genetic susceptibility locus for coronary heart disease and periodontitis. PLoS Genet. 2009; 5:e1000378. [PubMed: 19214202]

Silver N, Best S, Jiang J, Thein S. Selection of housekeeping genes for gene expression studies in human reticulocytes using real-time PCR. BMC Molecular Biology. 2006; 7:33. [PubMed: 17026756]

Trepagnier CM, Madden RM, Lazzari EP. Quantitative study of sodium hypochlorite as an in vitro endodontic irrigant. J Endod. 1977; 3:194–196. [PubMed: 266029]

Wilensky A, Polak D, Awawdi S, Halabi A, Shapira L, Houri-Haddad Y. Strain-dependent activation of the mouse immune response is correlated with Porphyromonas gingivalis-induced experimental periodontitis. J Clin Periodontol. 2009; 36:915–921. [PubMed: 19735468]

Wolff B, Berger T, Frese C, Max R, Blank N, Lorenz HM, Wolff D. Oral status in patients with early rheumatoid arthritis: a prospective, case-control study. Rheumatology (Oxford). 2014; 53:526–531. [PubMed: 24273047]

Wright HL, McCarthy HS, Middleton J, Marshall MJ. RANK, RANKL and osteoprotegerin in bone biology and disease. Curr Rev Musculoskelet Med. 2009; 2:56–64. [PubMed: 19468919]

Xiao YT, Xiang LX, Shao JZ. Vacuolar H(+)-ATPase. Int J Biochem Cell Biol. 2008; 40:2002–2006. [PubMed: 17897871]

Xu H, Zhang L, Gu L, Lu L, Gao G, Li W, Xu G, Wang J, Gao F, Xu JY, Yao J, Wang F, Zhang J, Xu GT. Subretinal delivery of AAV2-mediated human erythropoietin gene is protective and safe in experimental diabetic retinopathy. Invest Ophthalmol Vis Sci. 2014; 55:1519–1530. [PubMed: 24508793]

Yang DQ, Feng S, Chen W, Zhao H, Paulson C, Li YP. V-ATPase subunit ATP6AP1 (Ac45) regulates osteoclast differentiation, extracellular acidification, lysosomal trafficking, and protease exocytosis in osteoclast-mediated bone resorption. J Bone Miner Res. 2012; 27:1695–1707. [PubMed: 22467241]

Yang S, Chen W, Stashenko P, Li YP. Specificity of RGS10A as a key component in the RANKL signaling mechanism for osteoclast differentiation. J Cell Sci. 2007; 120:3362–3371. [PubMed: 17881498]

Yang S, Hao L, McConnell M, Zhou X, Wang M, Zhang Y, Mountz JD, Reddy M, Eleazer PD, Li YP, Chen W. Inhibition of Rgs10 Expression Prevents Immune Cell Infiltration in Bacteria-induced Inflammatory Lesions and Osteoclast-mediated Bone Destruction. Bone Res. 2013; 1:267–281. [PubMed: 24761229]

Zhang Q, Chen B. Interleukin-10 inhibits bone resorption: a potential therapeutic strategy in periodontitis and other bone loss diseases. 2014:284836. **2014**.

Zhao B, Ivashkiv LB. Negative regulation of osteoclastogenesis and bone resorption by cytokines and transcriptional repressors. Arthritis Res Ther. 2011; 13:234. [PubMed: 21861861]

Clinical Relevance

Scientific rationale for the study

Ac45 is the key subunit of the osteoclast proton pump, which is essential to osteoclast function. AAV is an effective tool of gene therapy. The disease features of bone resorption and inflammation of periodontitis led us to hypothesize that AAV-mediated Ac45 knock down may efficiently prevent periodontal tissue damage and alveolar bone loss.

Principal findings

Ac45 knockdown impaired extracellular acidification and osteoclast-mediated bone resorption, and local administration of AAV-sh-Ac45 into the periodontal lesions protected mice from periodontal bone erosion and attenuated inflammation, reduced T-cells, dendritic cells, macrophage infiltration and inhibited the expression of pro-inflammatory cytokines.

Practical implications

AAV-mediated Ac45 knockdown can be employed as a novel and effective periodontitis therapy.

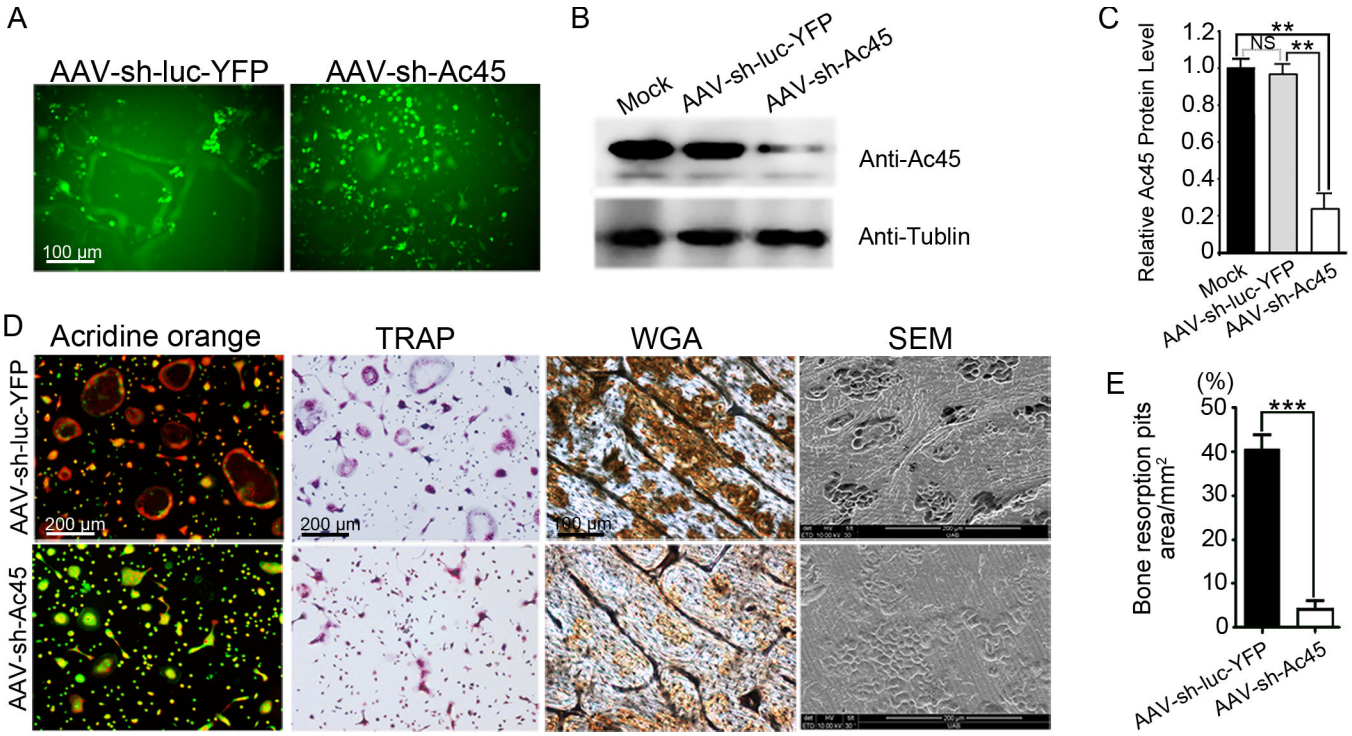

Figure. 1. AAV-sh-Ac45 efficiently knocked down expression of Ac45 and impaired osteoclast-mediated extracellular acidification and bone resorption *in vitro*

(**A**) Immunofluorescence photomicrograph of AAV-sh-luc-YFP and AAV-sh-Ac45 treatment groups 7 days after transduction. **(B)** Western blot of Ac45 expression in mouse bone marrow (MBM) transduced with AAV-sh-luc-YFP or AAV-sh-Ac45 or Mock (untreated). **(C)** Quantification of western blot. **(D)** Acridine orange staining of osteoclasts including cells without fusion (< 3 nuclei). TRAP stain, WGA to stain exposed bone matrix proteins and bone resorption pits visualized by scanning electron microscopy (SEM). **(E)** Quantification of SEM bone pits. N, S: No Significance. **, $P<0.01$, ***, $P<0.001$.

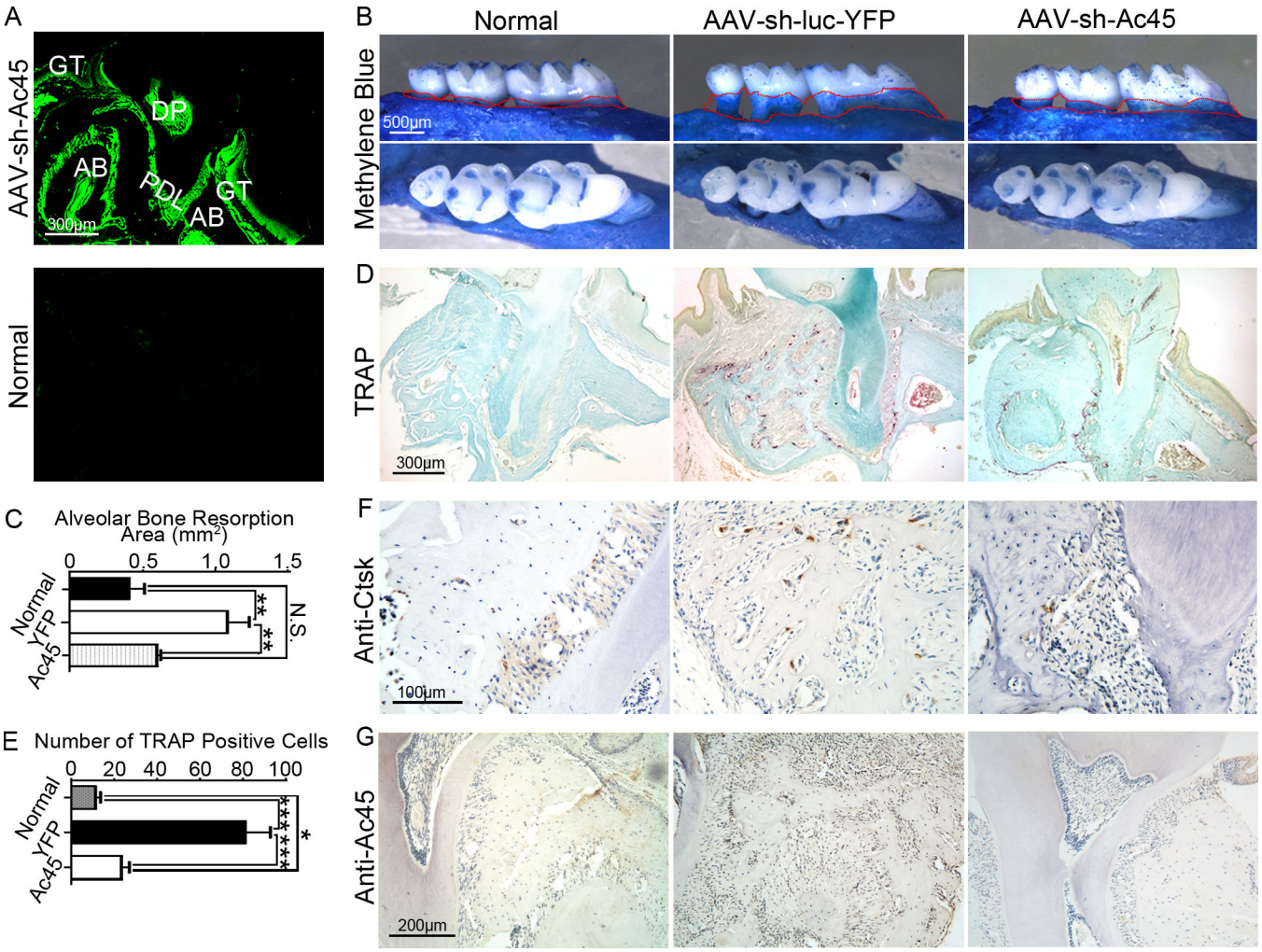

Figure. 2. AAV effectively transduced periodontal tissue and down regulated Ac45 expression leading to reduction of bone resorption in *P. gingivalis W50*-stimulated periodontitis

(A) The fluorescence microscope image revealing local delivery of AAV-sh-Ac45 resulted in EGFP expression in gingival tissue, tooth (T), periodontal ligament (PDL), dental pulp (DP), gingival tissue (GT), and alveolar bone (AB). **(B)** Representative figures from periodontal disease as indicated by alveolar bone loss and root exposure examined by Methylene blue staining. **(C)** Quantification analysis of the alveolar bone resorption area in periodontal lesion. **(D)** TRAP staining of periodontal area. **(E)** Quantification analysis of TRAP positive cell number in periodontal area. **(F)** Representative figures from anti-Ctsk immunohistochemistry staining of alveolar sections. **(G)** Representative figures from anti-Ac45 immunohistochemistry staining of alveolar sections. N, S: No Significance. *, $P<0.05$, **, $P<0.01$, ***, $P<0.001$.

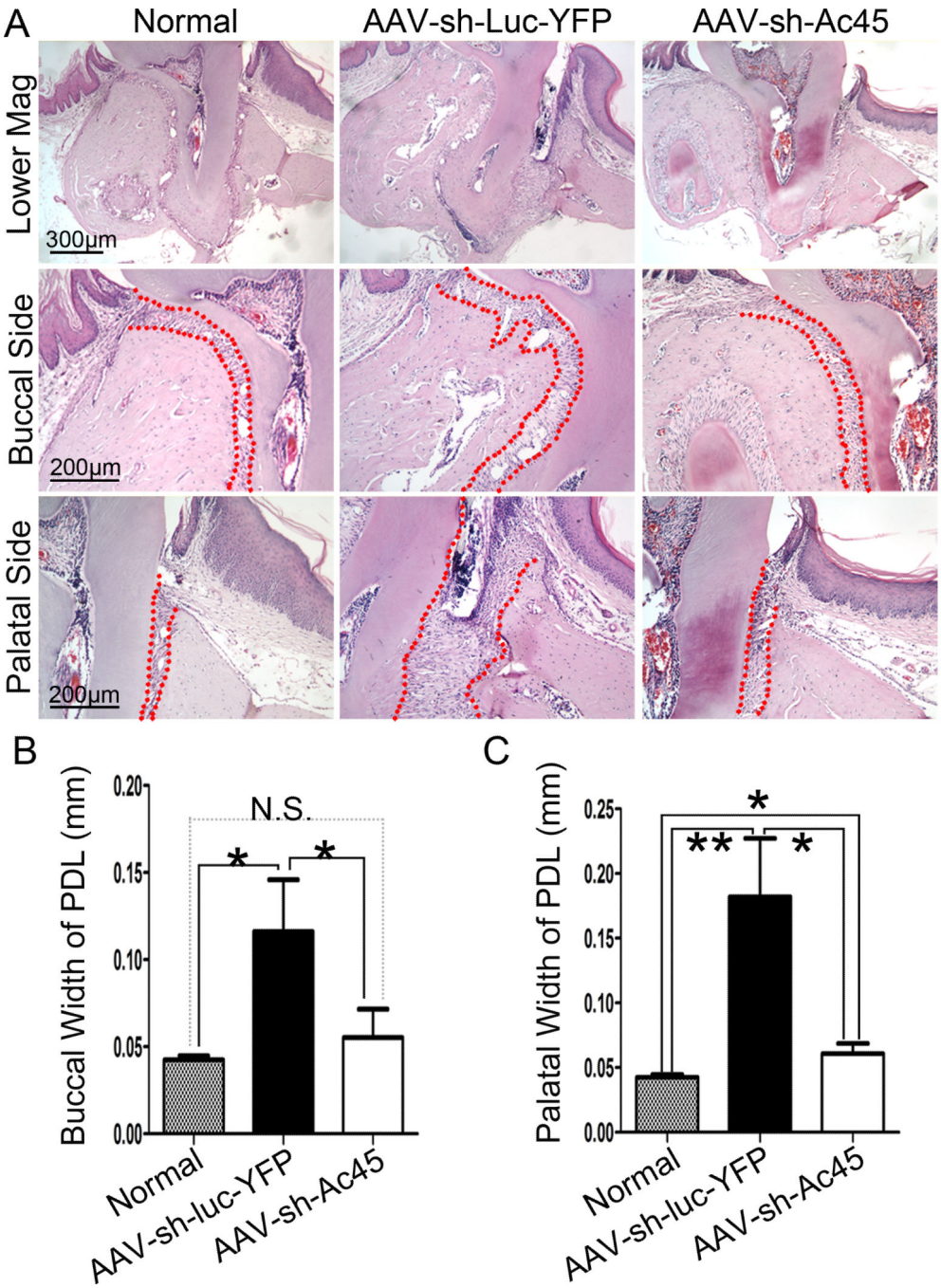

Figure. 3. AAV-mediated Ac45 knockdown decreased alveolar bone erosion and the width of periodontal ligament (PDL)

(**A**) Representative figures from hematoxylin & eosin staining of sections from uninfected mice (normal) or *P. gingivalis W50*-infected mice treated with AAV-sh-Ac45 or AAV-sh-luc-YFP. Mag indicates magnification. (**B**) The quantitative analysis of buccal width of PDL between the tooth root surface and the alveolar bone. (**C**) The quantitative analysis of palatal width of PDL. PDL: Periodontal Ligament. N, S: No Significance. *, $P<0.05$, **, $P<0.01$.

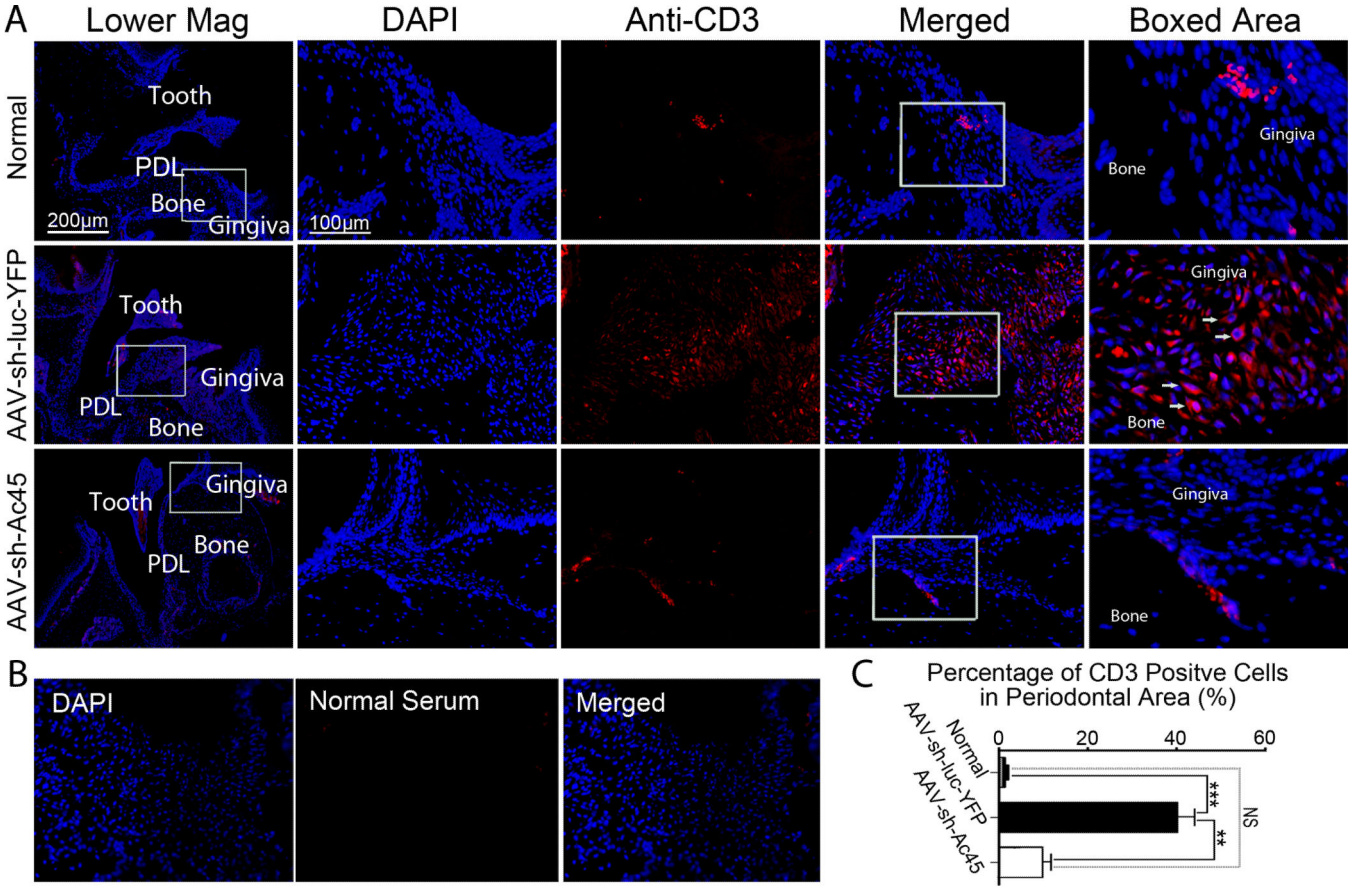

Figure. 4. AAV-mediated Ac45 knockdown decreases the number of T-cells in the periodontal lesion

(A) Representative figures from anti-CD3 immunofluorescence staining of alveolar sections. Cell nuclei were labeled using DAPI DNA stain (blue). (B) Negative control for anti-CD3 immunofluorescence staining, using normal serum instead of primary antibody. (C) Quantification analysis of percentage of CD3 positive T cells in periodontal area. GT: gingival tissue; AB: alveolar bone; PDL: periodontal ligament; T: teeth. N, S: No Significance. **, $P<0.01$, ***, $P<0.001$.

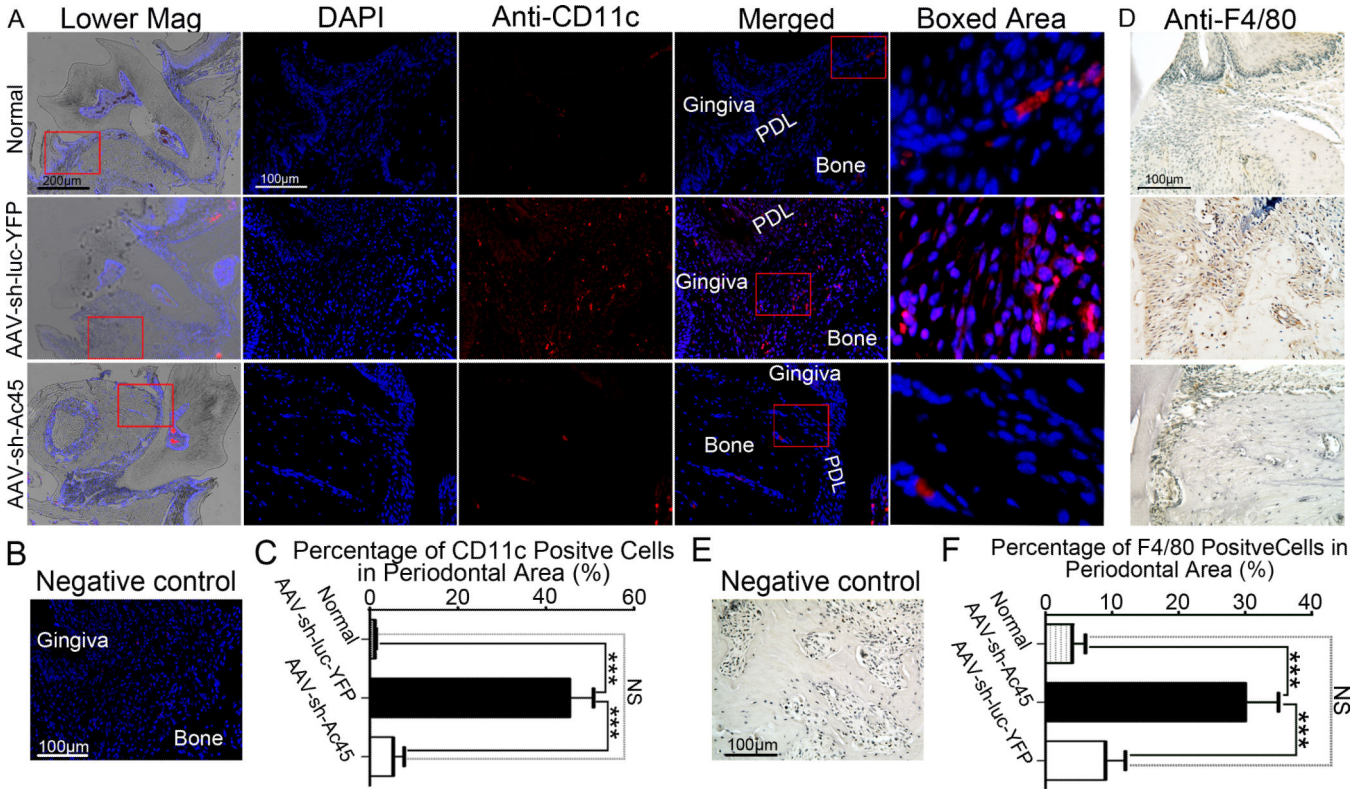

Figure. 5. AAV-mediated Ac45 knockdown decreased the number of dendritic cells and macrophages in the periodontal lesion

(A) Representative figures from anti-CD11c immunofluorescence staining of alveolar sections. Cell nuclei were labeled using DAPI DNA stain (blue). **(B)** Negative control for anti-CD11c immunofluorescence staining. **(C)** Quantification analysis of percentage of CD11c positive T cells in periodontal area. **(D)** Representative figures from anti-F4/80 immunohistochemistry staining of alveolar. **(E)** Negative control for anti-F4/80 immunohistochemistry staining. **(F)** Quantification analysis of percentage of F4/80 positive macrophages in periodontal area. GT: gingival tissue; AB: alveolar bone; PDL: periodontal ligament; T: teeth. N, S: No Significance. ***, *P*<0.001.

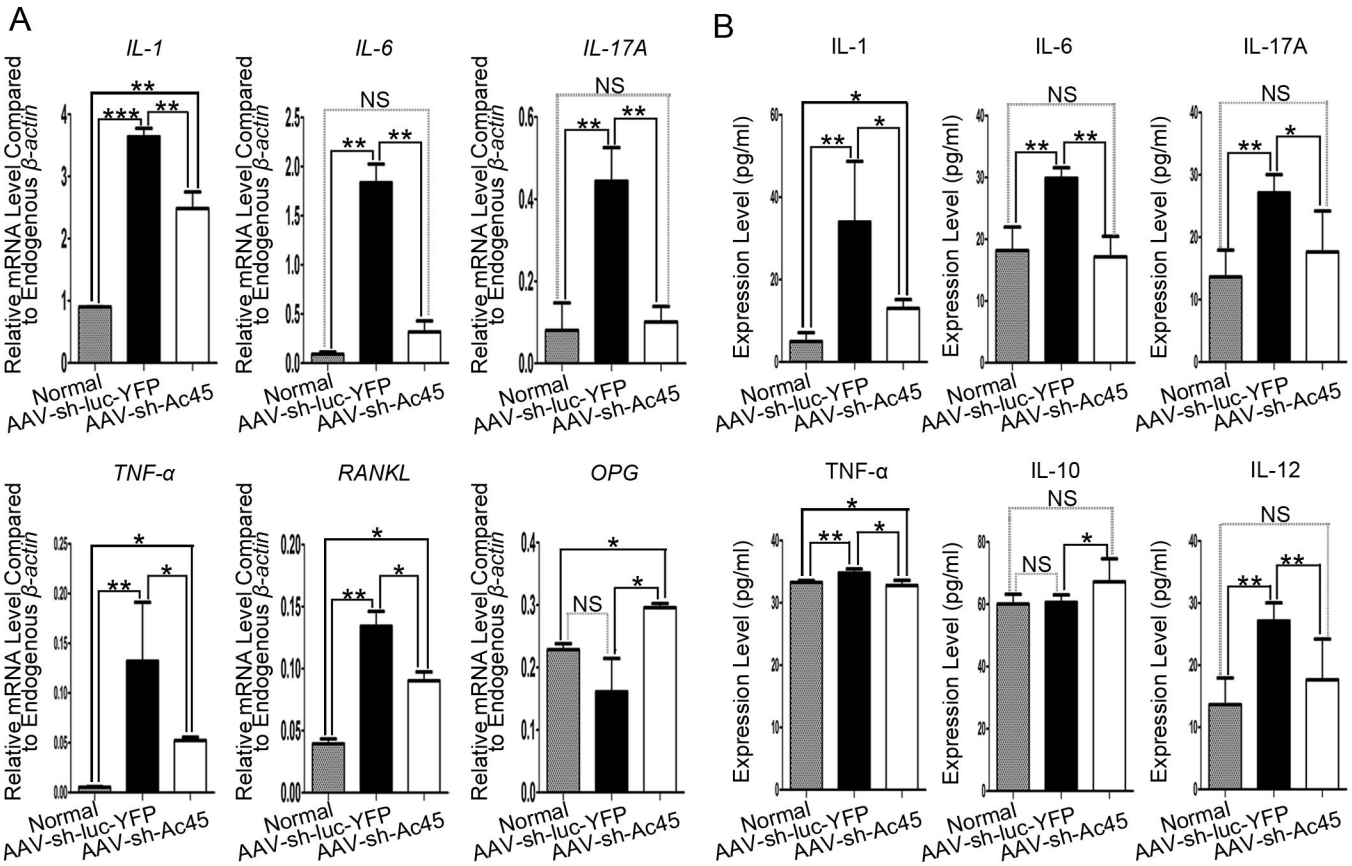

Figure. 6. AAV-sh-Ac45 reduced the expression of pro-inflammatory cytokines in the periodontal tissues

(A) qRT-PCR of pro-inflammatory cytokines (*i.e. IL-1α, IL-6, TNF-α, IL-17A*) and *RANKL* and *OPG* in the periodontal tissues. Expression levels were normalized to β-actin (pooled 5 samples each time in each group on three independent experiments). (B) *IL-1α, IL-6, TNF-α, IL-10, IL-12 and IL-17A* levels in the periodontal tissues as detected by ELISA. N, S: No Significance. *, $P<0.05$, **, $P<0.01$, ***, $P<0.001$.